

RESEARCH

Open Access



Novel Plastic Hinge Element for Seismic Performance Assessment of RC Bridge Columns with Lap Splices

Tae-Hoon Kim^{1*} , Ki-Young Eum¹ and Hyun Mock Shin²

Abstract

This paper presents a nonlinear analysis procedure for evaluating the seismic performance of reinforced concrete (RC) bridge columns with lap splices using a novel plastic hinge element considering shear deformation. To accurately assess the inelastic behavior of RC bridge columns, reliable three-dimensional (3D) constitutive models are required. However, developing a 3D nonlinear material model is difficult and computationally intensive. In this study, to address these issues, a new plastic hinge element considering shear deformation for RC bridge columns is developed. The new plastic hinge element is based on the Timoshenko beam theory and utilizes two-noded zero length element with six degrees of freedom. The finite element model was implemented in a computer program named Reinforced Concrete Analysis in Higher Evaluation System Technology (RCAHEST) developed by the authors. The developed plastic hinge element for seismic performance assessment of RC bridge columns with lap splices was validated through comparison of the numerical and experimental results.

Keywords: nonlinear analysis, plastic hinge element, seismic performance assessment, bridge columns, lap splices

1 Introduction

In reinforced concrete (RC) bridge columns with lap splices, inelastic deformations generally occur over a finite hinge length (Aboutaha et al., 1999). The spread of hinge length is a critical factor in the deformation analysis of RC bridge columns and includes elastic, plastic, and softening stages of response (Alemdar, 2010; Bae & Bayrak, 2014).

The required confined zone of bridge columns under lateral sway during earthquakes is related to the plastic hinge length. The inelastic curvatures in the plastic hinges are assumed to be constant across its entire length, to simplify the estimation of the displacement at

the end of the bridge column (Bae & Bayrak, 2014; Fedak, 2012).

The lumped plasticity method leverages the simplicity of the plastic hinge by separating a line element into inelastic and elastic components. The distributed plasticity formulation has received attention for its ability to account for the nonlinear behavior along the element length (Caltrans, 2010).

The ultimate response of RC bridge columns, particularly the existing shear deficient designed according to old design codes, is affected by shear failure in many cases. Recent studies have attempted to overcome this limitation by introducing the Timoshenko beam theory into the fiber approach, or even a generalized beam theory incorporating multi-axial constitutive laws (Bentz et al., 2006; Han et al., 2014; Marini & Spacone, 2006; Michelini et al., 2017; Zendaoui et al., 2016).

In deriving the section kinematics equations, Timoshenko beam theory has been used to account for shear deformations. The efficiency and accuracy of the

*Correspondence: thkim@krii.re.kr

¹ Advanced Railroad Civil Engineering Division, Korea Railroad Research Institute, 176, Cheoldobangmulgwan-Ro, Uiwang-Si 16105, Gyeonggi-Do, Korea
Full list of author information is available at the end of the article

mixed-based formulation were assessed by examining the global and local level responses under monotonic and cyclic loadings and by reproducing experimentally observed failure modes (Das & Ayoub, 2021). In particular, fiber-based beam elements are able to describe the nonlinear behaviors along the depth by discretizing the cross section into several fibers with a reasonable constitutive law (Mullapudi & Ayoub, 2010, 2018; Xu et al., 2020).

The aim of this study is to evaluate the seismic performance of RC bridge columns using a new plastic hinge element with beam-column element. To account for the shear deformation effect, the proposed numerical method was applied to the hinge model along with the nonlinear shear response history constitutive law for the section.

Nonlinear shear response hysteretic law for the section was obtained from the shear force versus shear strain relationship as a member based on the concept of average strain. The design shear strength presented in the Korea Bridge Design Code (Limit State Design Method) (MCT, 2012) based on the reliability-based limit state design was applied. This model is practical and conservative. A new tri-linear fracture envelope curve incorporating the concrete shear crack strength, yielding stress of shear reinforcement, tension stiffening effect of shear reinforcement, and the concrete compression strut angle of inclination of the θ_s was proposed. The additional confinement effect at the joint of the foundation of RC bridge columns and axial force, the tensile steel ratio, and the span-to-depth ratio are reflected in the calculation of the concrete compression angle.

Experimentally evaluating the seismic performance of such RC structures is expensive, time consuming, and tedious. In this paper, a simple new plastic hinge element is proposed for the analysis of RC bridge columns. A computer program Reinforced Concrete Analysis in Higher Evaluation System Technology (RCAHEST), developed by the authors (Kim et al., 2003, 2006, 2009, 2014, 2022), was modified to include a plastic hinge element considering shear deformation.

2 Nonlinear Finite Element Analysis Program, RCAHEST

To accurately assess the seismic performance of RC bridge columns with lap splices, reliable three-dimensional (3D) constitutive models are required. However, developing a 3D nonlinear material model is difficult and computationally intensive. The main problems are the extensive amounts of computer storage required for an accurate solution (Cerioni et al., 2011; Kim et al., 2014, 2022; Mirzabozorg & Ghaemian, 2005; Mourlas et al., 2017; Spiliopoulos & Lykidis, 2006).

Therefore, a new simple plastic hinge element considering the shear deformation of RC bridges columns with lap splices is developed in this study. The model was developed and analyzed using RCAHEST (Kim et al., 2003, 2006, 2009, 2014, 2022). The proposed structural element library RCAHEST is built based on the finite element analysis program called FEAP, developed by Taylor (2000).

The nonlinear finite element model of RC consists of models describing the behavior of the concrete and reinforcement.

Concrete models can be composed of cracked concrete and uncracked concrete. Cracked concrete is divided into three models in the direction normal to the crack plane, direction of the crack plane, and in the shear direction at the crack plane (see Fig. 1). The basic crack model is based on the nonorthogonal fixed crack method of the smeared crack approach (Moshirabadi & Soltani, 2019; Vecchio, 2000; Zhu et al., 2001).

A refined tension stiffness model is obtained by transforming the tensile stresses of concrete into the component normal to the crack, and improved accuracy is expected. A modified elasto-plastic fracture model is used to describe the compressive behavior of concrete struts in between cracks in the direction of the crack plane. The shear transfer model is used to consider the effect of shear stress transfer due to the aggregate interlock at the crack surface.

The post-yield constitutive law of reinforcement in concrete considers the bond characteristics, and the model is a bilinear model. Considering the buckling of reinforcing bars, it is assumed that the average stress-strain behavior after concrete crushing decreases linearly until it reaches 20% of the average reinforcement stress (Kim et al., 2003). The transverse reinforcing bars confine the compressed concrete in the core region and reduce the buckling of the longitudinal reinforcements. In addition, the transverse reinforcing bars improve the

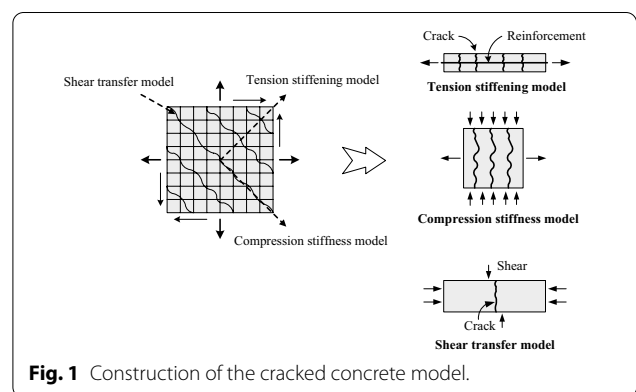


Fig. 1 Construction of the cracked concrete model.

ductility capacity of the unconfined concrete. In the case of the laterally confined core concrete, the analysis model should properly consider the out of plane stress, which is a shortcoming of two-dimensional analysis, triggered by the volumetric expansion of concrete. Many researchers have suggested empirical or semi-empirical models to evaluate such confining effect. In this study, the model proposed by Mander et al. (1988) is adopted in the analysis model as the equivalent stress–strain relation for concrete. The Mander’s model expresses the normalized stress–strain relationship of confined and unconfined concrete as a function of the cross-sectional shape, the arrangement of reinforcement, and the material strength. The modified confined model was applied in advance before the finite element method analysis to correct the strain–stress curve of the two-dimensional model. The equations also consider the yield strength, the distribution type, and the amount of the longitudinal and transverse reinforcing bars for the computation of the effective lateral confining stress and the ultimate compressive strength and strain of the confined concrete. The authors (Kim et al., 2003, 2006, 2009, 2014, 2022) have modified the peak confined strength in Mander’s model for the flexural analysis and predicted the behavior of columns under flexure reasonably well.

An RC bridge column with lap splices at the maximum moment section can lose its load resistance due to splice bond failure (Darwin et al., 1996; Kim et al., 2006). The subsequent response is characterized by extremely narrow energy dissipation loops and rapid strength degradation. A developed bond stress–slip relationship can be idealized for a bar subjected to cyclic loading (see Fig. 2) (Kim et al., 2006). The maximum bond stress, $\tau_{b,max}$, that can be developed is a function of the intensity of the reversed loading and the range of that loading.

A complete description of the nonlinear RC model is provided by Kim et al., (2003, 2006, 2009, 2014, 2022).

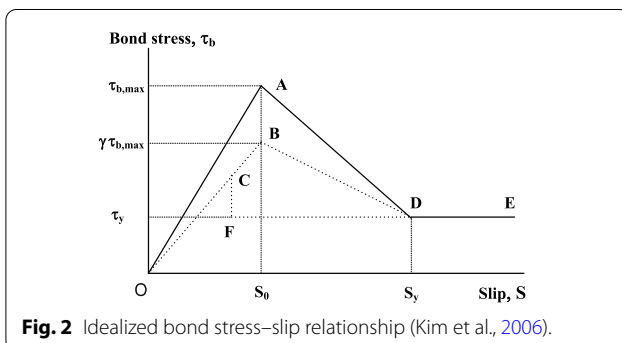


Fig. 2 Idealized bond stress–slip relationship (Kim et al., 2006).

3 Development of Plastic Hinge Element Considering Shear Deformation

3.1 Overview

The lumped plasticity model assumes that all inelastic actions are concentrated in a single point or region, termed the plastic hinge length. This representation simplifies the actual curvature distribution into plastic and elastic regions (see Fig. 3). Similar to the case of curvature, the ultimate displacement can be defined by the sum of plastic and elastic components, as shown in Fig. 4 (Fedak, 2012):

$$\Delta_u = \Delta_y + \Delta_p, \tag{1}$$

where Δ_u is the ultimate displacement, Δ_y is the yield displacement, and Δ_p is the plastic displacement.

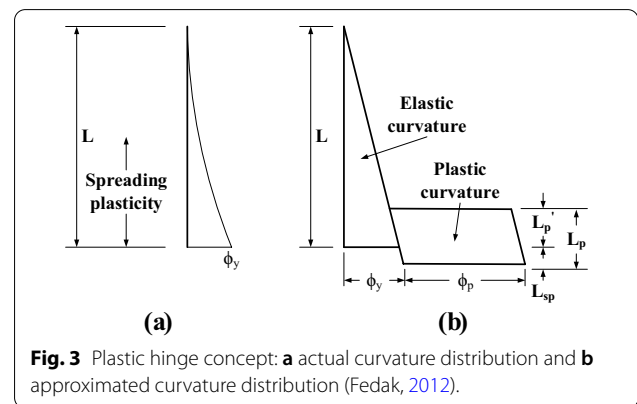


Fig. 3 Plastic hinge concept: **a** actual curvature distribution and **b** approximated curvature distribution (Fedak, 2012).

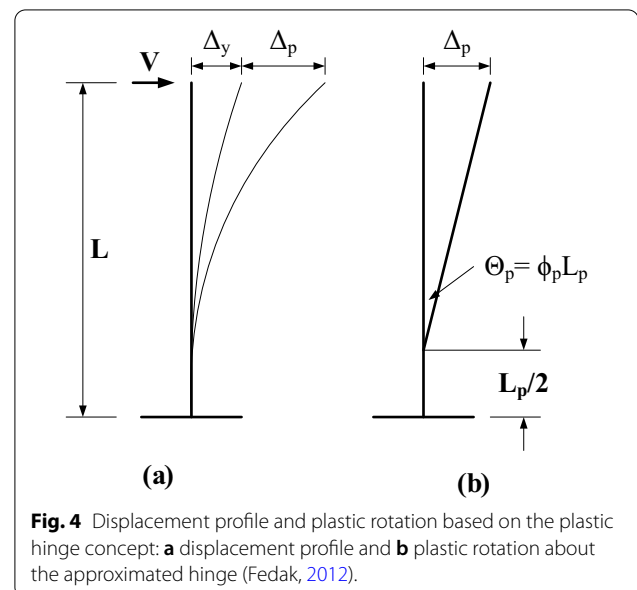


Fig. 4 Displacement profile and plastic rotation based on the plastic hinge concept: **a** displacement profile and **b** plastic rotation about the approximated hinge (Fedak, 2012).

The yield and plastic displacements are a function of the plastic hinge components and the sectional response quantities:

$$\Delta_y = \frac{\phi_y(L + L_{sp})^2}{3}, \tag{2}$$

$$\Delta_p = (\phi_u - \phi_y)L_p H, \tag{3}$$

$$H = L - L_p/2, \tag{4}$$

where L_p is the height of the plastic portion, L'_p is the plastic curvatures above the column base, and L_{sp} is the length of strain penetration inside the foundation.

Estimation of the plastic hinge length formed in RC bridge columns is complicated using sophisticated non-linear analysis program. The plastic hinge length depends on many factors: (1) axial load level, (2) moment gradient, (3) shear stress level, (4) mechanical properties of reinforcement, (5) concrete strength, and (6) confinement level and its effectiveness (Bae & Bayrak, 2014).

For the plastic hinge model, numerical methods can generally be divided into two categories: lumped plasticity and distributed plasticity. At the early stages of damage, the lumped plasticity method tends to provide more accurate comparison in terms of the experimental hysteretic behavior. The lumped plasticity approach is advantageous owing to its simplicity. Distributed plasticity methods are more accurate than lumped methods because it is physically impossible to incorporate a lumped element. Therefore, the distributed method more accurately considers the plasticity spread along an element (Fedak, 2012).

3.2 Formulation for Plastic Hinge Element

The developed plastic hinge elements are located at either end of an element and utilize a two-noded zero length element with six degrees of freedom. It could be used at the bottom of the element at the column base for bridge columns. This element is used to analyze element behavior through displacement-based formulation.

The proposed model for understanding shear behavior is based on the Timoshenko beam theory. It conceptualizes shear behavior as the average shear deformation.

The element force vector and displacement vector are as follows:

$$\bar{Q} = \{\bar{Q}_1, \bar{Q}_2, \bar{Q}_3, \bar{Q}_4, \bar{Q}_5, \bar{Q}_6, \bar{Q}_7, \bar{Q}_8, \bar{Q}_9, \bar{Q}_{10}, \bar{Q}_{11}, \bar{Q}_{12}\}^T, \tag{5}$$

$$\bar{q} = \{\bar{q}_1, \bar{q}_2, \bar{q}_3, \bar{q}_4, \bar{q}_5, \bar{q}_6, \bar{q}_7, \bar{q}_8, \bar{q}_9, \bar{q}_{10}, \bar{q}_{11}, \bar{q}_{12}\}^T. \tag{6}$$

The section forces and corresponding section deformations are as follows:

$$D(x) = \begin{Bmatrix} N(x) \\ M_y(x) \\ M_z(x) \end{Bmatrix} = \begin{Bmatrix} D_1(x) \\ D_2(x) \\ D_3(x) \end{Bmatrix}, \tag{7}$$

$$d(x) = \begin{Bmatrix} \varepsilon(x) \\ \kappa_y(x) \\ \kappa_z(x) \end{Bmatrix} = \begin{Bmatrix} d_1(x) \\ d_2(x) \\ d_3(x) \end{Bmatrix}. \tag{8}$$

The cross-sectional deformation vector increments and force vector increments can be represented as follows:

$$\Delta d(x) = B(x)\Delta \bar{q}, \tag{9}$$

$$\Delta D(x) = k_t(x)\Delta d(x). \tag{10}$$

where $B(x)$ is the displacement shape function and $k_t(x)$ is the cross-sectional tangent stiffness matrix.

Equilibrium equations can be obtained based on the virtual work principle. The element tangent stiffness and the increment of the element resisting forces (ΔQ_R) are obtained as follows:

$$\bar{\delta q}^T \Delta \bar{Q} = \int_0^L \delta d^T \Delta D(x) dx, \tag{11}$$

$$\bar{K}_t = \int_0^L B^T(x) k_t(x) B(x) dx, \tag{12}$$

$$\Delta Q_R = \int_0^L B^T(x) \Delta D_R(x) dx. \tag{13}$$

The element nodal displacement increments and corresponding tangent stiffness are as follows:

$$\Delta u = T_e^T \Delta \bar{q}, \tag{14}$$

$$K_{et} = T_e^T \bar{K} T_e, \tag{15}$$

where T_e is the element coordinate transformation matrix.

The plastic hinge element considering shear deformation is considered as the boundary elements at the column base. Accordingly, the stiffness matrix of plastic hinge element in the local coordinate system is as follows:

$$\{p_s\} = [k_s] \{d_s\} \tag{16}$$

where $\{p_s\}$ is the load vector, $[k_s]$ is the stiffness matrix, and $\{d_s\}$ is the displacement vector.

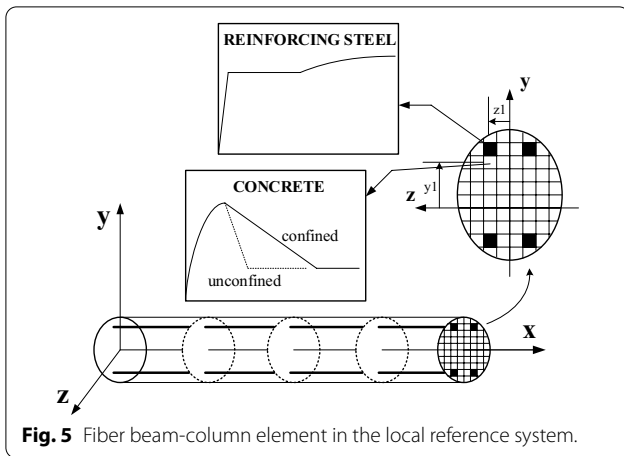


Fig. 5 Fiber beam-column element in the local reference system.

3.3 Nonlinear Material Model for Plastic Hinge Element

The new formulation was developed for determining the section state, and the shear constitutive model was implemented into a fiber plastic hinge element.

The strains and stresses of the i th fiber are related by the following relationship (see Fig. 5):

$$e(x) = \begin{Bmatrix} \varepsilon_1(x, y_1, z_1) \\ \vdots \\ \varepsilon_{ifib}(x, y_{ifib}, z_{ifib}) \\ \vdots \\ \varepsilon_n(x, y_n, z_n) \end{Bmatrix}, \tag{17}$$

$$E(x) = \begin{Bmatrix} \sigma_1(x, y_1, z_1) \\ \vdots \\ \sigma_{ifib}(x, y_{ifib}, z_{ifib}) \\ \vdots \\ \sigma_n(x, y_n, z_n) \end{Bmatrix}. \tag{18}$$

Nonlinear shear response hysteretic law for the section is obtained from the shear force versus shear strain relationship as a member based on the average strain concept for the section.

The design shear strength presented in the Korea Bridge Design Code (Limit State Design Method) (MCT, 2012) that is based on the reliability-based limit state design was applied. This method is similar to Eurocode 2 (CEN, 2004). Since the purpose of this program is to design practical maintenance of reinforced concrete bridge columns, it is possible to design safer maintenance by using a rather conservative model that is generally applied in design for shear failure. A new tri-linear fracture envelope curve presenting the concrete shear crack strength, yielding stress of shear

reinforcement, tension stiffening effect of shear reinforcement, and the concrete compression strut angle of inclination of the θ_s was proposed (see Fig. 6).

On the curve, there are three parts with three different slopes. The first part with a linear portion OA and slope (G_c) shows the uncracked behavior of RC and connects the origin point O to the point A (γ_c, V_c). The point A is associated with the stress state at which the nominal principal tensile stress reaches the nominal tensile strength of concrete. In order to calculate the shear strength without shear reinforcement V_c , the uncracked shear slope (G_c), and the Korea Bridge Design Code (Limit State Design Method) (MCT, 2012), the following expressions are used:

$$V_c = \left[0.85\phi_c\kappa(\rho f_{ck})^{1/3} + 0.15f_n \right] b_w d, \tag{19}$$

$$\gamma_c = \kappa \frac{V_c}{G_c A_c}, \tag{20}$$

$$G_c = \frac{E_c}{2.3} = \frac{8,500(\sqrt{f_{ck}})^{1/3}}{2.3}, \tag{21}$$

where V_c is the shear strength without shear reinforcement, ϕ_c is the concrete material resistance factor, κ is the shear coefficient, ρ is the $A_s/(b_w d)$, f_{ck} is the characteristic value of cylindrical compressive strength, f_n is the $N_u/A_c \leq 0.2\Phi_c f_{ck}$, N_u is the axial force due to factored load, A_c is the cross-sectional area, b_w is the web width of section, d is the effective depth of section, γ_c is the shear strain, G_c is the shear elastic modulus of concrete, and E_c is the elastic modulus of concrete.

The second part with a linear portion AB and slope (G_d) represents the sectional shear response between

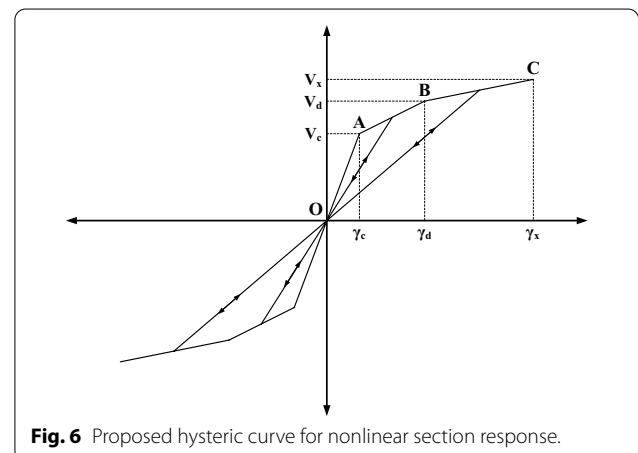


Fig. 6 Proposed hysteretic curve for nonlinear section response.

point A (γ_c, V_c) and point B (γ_d, V_d). Point B is detected based on the fiber-section model:

$$V_d = \frac{\phi_s f_{vy} A_v z}{s} \cot \theta_s \geq \frac{\phi_c v f_{ck} b_w z}{\cot \theta_s + \tan \theta_s} = V_{d,max}, \quad (22)$$

$$\gamma_d = 2(\bar{\varepsilon}_y + \varepsilon_{2,d}) \tan \theta_s, \quad (23)$$

$$\varepsilon_{2,d} = \left(1 - \sqrt{\frac{(V_{d,max} - V_d)}{V_{d,max}}} \right) \varepsilon_{cu}, \quad (24)$$

$$G_d = \frac{V_d - V_c}{\gamma_d - \gamma_c}, \quad (25)$$

where V_d is the shear strength with shear reinforcement, ϕ_s is the steel material resistance factor, f_{vy} is the yield strength of shear reinforcement, A_v is the cross-sectional area of shear reinforcement, z is the internal arm length along the span, s is the spacing of stirrups, θ_s is the angle of strut, v is the strength reduction factor for concrete cracked in shear, γ_d is the shear strain with shear reinforcement, $\bar{\varepsilon}_y$ is the average yielding strain of shear reinforcement, $\varepsilon_{2,d}$ is the strain of compressive strut with shear reinforcement, ε_{cu} is the ultimate strain of concrete, and G_d is the slope of AB as shown in Fig. 6.

The third part with a linear portion BC features a slope (G_x) representing the sectional shear response between point B (γ_d, V_d) and point C (γ_x, V_x). To determine the maximum shear force considering tension stiffening, this study employs the follow equations proposed by authors. The shear strain at the onset of transverse reinforcement yielding γ_x can be determined based on the truss analogy approach:

$$V_x = \frac{\phi_s f_{vs} A_v z}{s} \cot \theta_s \geq \frac{\phi_c v f_{ck} b_w z}{\cot \theta_s + \tan \theta_s} = V_{d,max}, \quad (26)$$

$$\gamma_x = 2(3\bar{\varepsilon}_y + \varepsilon_{2,x}) \tan \theta_s, \quad (27)$$

$$\varepsilon_{2,x} = \left(1 - \sqrt{\frac{(V_{d,max} - V_x)}{V_{d,max}}} \right) \varepsilon_{cu}, \quad (28)$$

$$G_x = \frac{V_x - V_d}{\gamma_x - \gamma_d}, \quad (29)$$

where V_x is the maximum shear force considering tension stiffening, f_{vs} is the average maximum stress of shear reinforcement considering tension stiffening, γ_x is the shear strain considering tension stiffening, $\varepsilon_{2,x}$ is the strain of compressive strut considering tension stiffening, and G_x is the slope of BC as shown in Fig. 6.

4 Numerical Examples

4.1 Description of Test Specimens and Numerical Simulations

The data provided by Kim et al. (2006) for the RC bridge columns with lap splices are used to validate the applicability of the new plastic hinge element considering shear deformation.

The mechanical properties of the specimens are provided in Table 1 and the geometric details are shown in Fig. 7. All specimens tested were subjected to the constant axial load of $0.07f_{ck}A_c$.

Firstly, for comparison, Figs. 8 and 9 show the finite element discretization and the boundary conditions for plane stress analyses of the RC bridge column specimens.

Figures 8b and 9b show a method for transforming a circular section into rectangular strips for using the plane stress elements. For rectangular sections, the equivalent strips are calculated. The internal forces are calculated and subsequently the equilibrium is checked (Kim et al., 2006, 2009, 2014, 2022).

The refinement of the mesh is sufficient because the errors between the area and the moment of inertia of a circular section and those of an equivalent rectangular section are smaller than 3%. It is assumed in the analysis that the reinforcing bars are equally distributed in the concrete section.

To verify the applicability of the developed plastic hinge elements considering shear deformation, Fig. 10 shows the finite element discretization and the boundary conditions for plastic hinge analyses of the RC bridge columns with lap splices.

4.2 Comparison with Experimental Results

NS and FS series are the RC bridge column specimens, and the load–displacement curves of the specimens are shown in Figs. 11 and 12. Numerical results show suitable agreement with the experimental results.

The hysteresis curves show that the strength reduction is mainly owing to the degradation of the splice region. The failure modes are brittle due to rapid strength reduction following the debonding of longitudinal reinforcements.

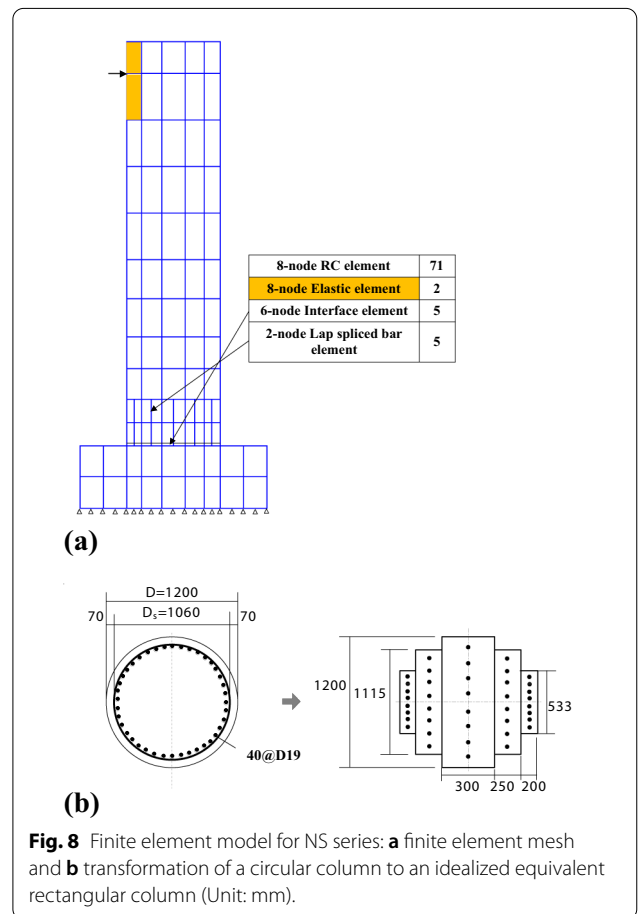
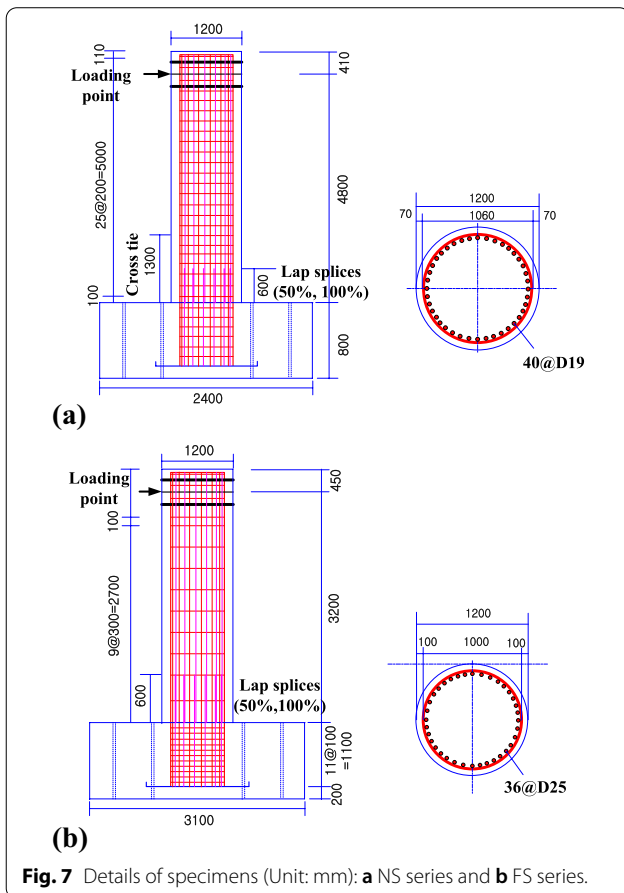
Both the experimental and numerical results show that the increase in the lap spliced ratio yields lower ductility. The specimens with 50% lap splices developed more ductility than the specimens with 100% lap splices. This occurs due to the longitudinal bars slip in the spliced region shortly after yielding in the reinforcing bars.

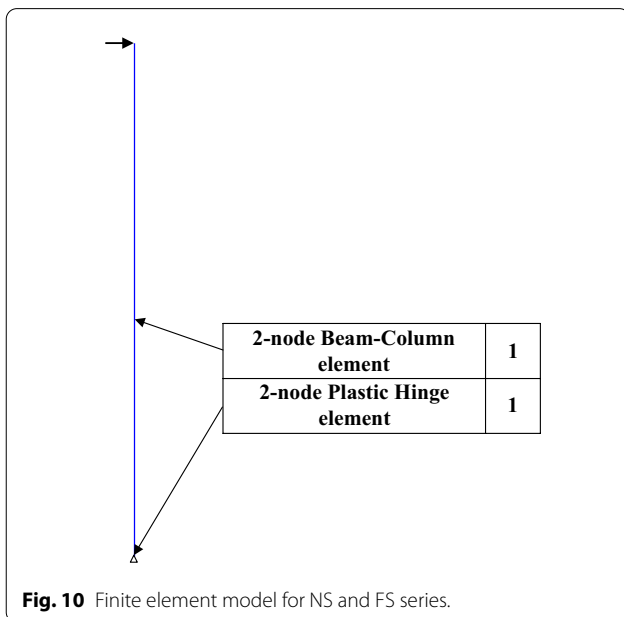
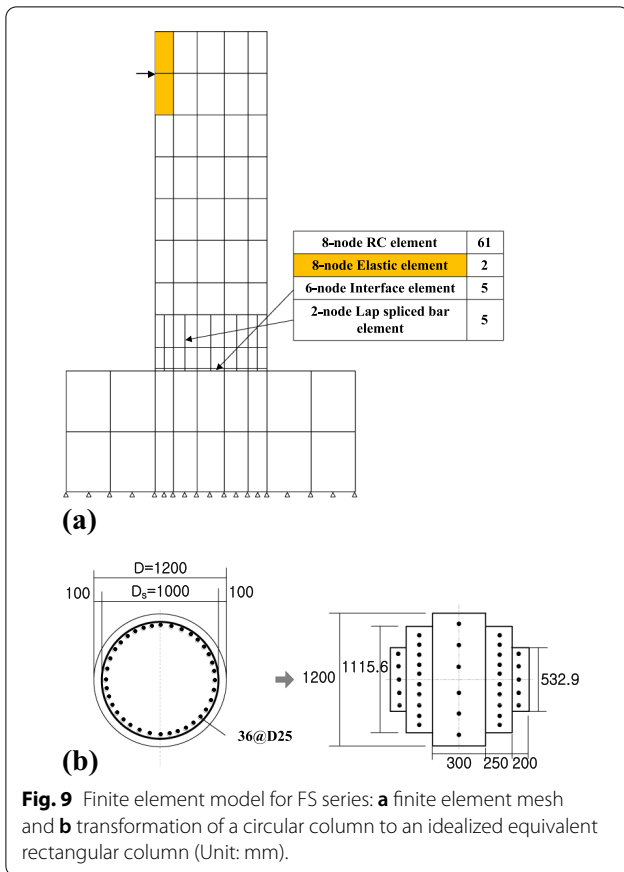
The values corresponding to all the column specimens were comparable to the numerical results (see Table 2). The calculated load capacities were usually lower than the experimental results. Seismic performance of RC

Table 1 Properties of the reinforced concrete column specimens.

Specimen		NS-HT2-H-L2	NS-HT2-A-L2	FS-H-LS050	FS-H-LS100
Diameter of cross section (mm)		1200		1200	
Effective height (mm)		4800		3200	
Aspect ratio		4.0		2.67	
Longitudinal reinforcement	Diameter	D19		D25	
	Yielding stress (MPa)	343.2		331.3	
	Reinforcement ratio (%)	1.01		1.60	
Transverse reinforcement	Diameter	D10		D13	
	Yielding stress (MPa)	372.7		326.2	
	Volumetric ratio (%)	0.127		0.340	
Strength of concrete (MPa)		24.8		24.5	
Axial load ratio ($\frac{P}{f_{ck}A_c}$)		0.07		0.07	
Lap spliced length (mm)		600		600	
Lap spliced ratio (%)		50	100	50	100

Lap spliced ratio of longitudinal reinforcement; details of reinforcement (see Fig. 1).



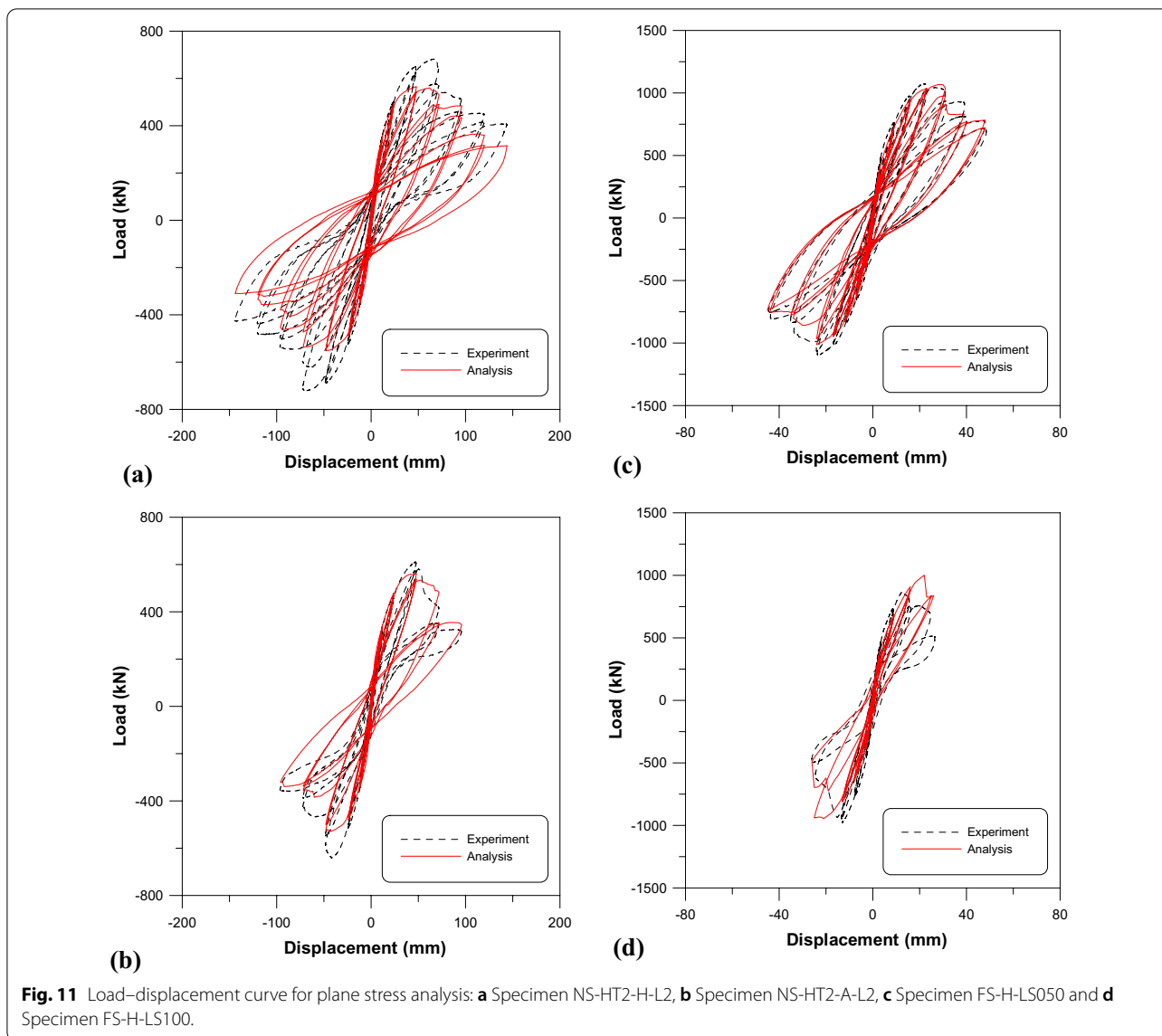


bridge columns with lap splices can be assessed based on displacement ductility. The displacement ductility is associated with flexural and shear carrying capacities. The experimental displacement ductility factors ranged from 3.0 to 2.0 and exhibited brittle behavior.

The results of four experiments were compared with those of the plane stress analysis and plastic hinge analysis. When employing plane stress analysis to predict the experimental results of the specimens, the average ratios of the experimental to numerical maximum strength were 1.04 at a CV of 14%. Average ratios of the experimental to numerical ductility factors were 1.20 at a CV of 34%. On the contrary, when using plastic hinge analysis to predict the results of the specimens, the average ratios of the experimental to numerical maximum strength were 1.03 at a CV of 14%. The average ratios of the experimental to numerical ductility factors were 0.83 at a CV of 21%. Comparisons with the experimental results show that the response prediction is significantly improved when the developed fiber–shear formulation is incorporated. Numerical results obtained using the proposed plastic hinge model are certainly promising, but the ductility is overestimated. Additional numerical studies are required to confirm and refine design details, particularly for practical or field use.

With respect to validity of the model, correlation studies between numerical and experimental responses of RC bridge columns with lap splices under cyclic loadings revealed that the proposed plastic hinge element could suitably resemble the salient features of the experimental force–displacement responses, including the shape of hysteretic response, the amount of dissipated hysteretic energy, and the member capacity. The sectional shear failure subsequent to plastic hinge formation can be accurately captured by the proposed displacement-based fiber model. This shear failure mode involving sectional shear deterioration and the rapid increase of the sectional shear strain subsequent to the plastic hinge formation appropriately complied with the experimental observation.

By using a developed plastic hinge element, the analysis time can be remarkably reduced, as shown in Table 3. The analysis time of plane stress elements is 359.58, 131.33, 217.72, and 70.75 s, respectively. On the contrary, the analysis time of fiber beam-column elements and plastic hinge elements is 59.71, 28.69, 36.39, and 13.88 s, respectively. Nonlinear finite element analysis was performed on the systems equipped with Intel(R) Core(TM) i7-8700 CPU@3.20 GHz and 8 GB memory. The proposed plastic hinge element proved to be considerably more computationally efficient than finite element programs using plane stress elements, but the computational times required by the plane stress models are acceptable.



5 Conclusions

A new plastic hinge element considering shear deformation for assessing the seismic performance of RC bridge columns with lap splices under earthquake was developed. Based on the results of the numerical examples, the following conclusions were drawn.

- With respect to validity of the proposed model, correlation studies between numerical and experimental responses of RC bridge columns under cyclic loadings revealed that the new plastic hinge element could suitably resemble the salient features of the experimental responses.
- The developed plastic hinge element proved to be considerably more computationally efficient than finite element programs owing to the use of plane stress elements. Comparisons with the experimental results showed that the response prediction was significantly improved upon incorporating the developed fiber–shear formulation.
- The proposed finite element analysis procedures describe the load–deformation responses, load capacities, and failure modes of the RC bridge columns with lap splices under earthquake with acceptable accuracy. From the comparisons of the predicted load–displacement responses with the measured responses, it is clear that the ductility of the bridge column specimens may be limited by the crushing of the concrete and by bond failure of the lap splices.

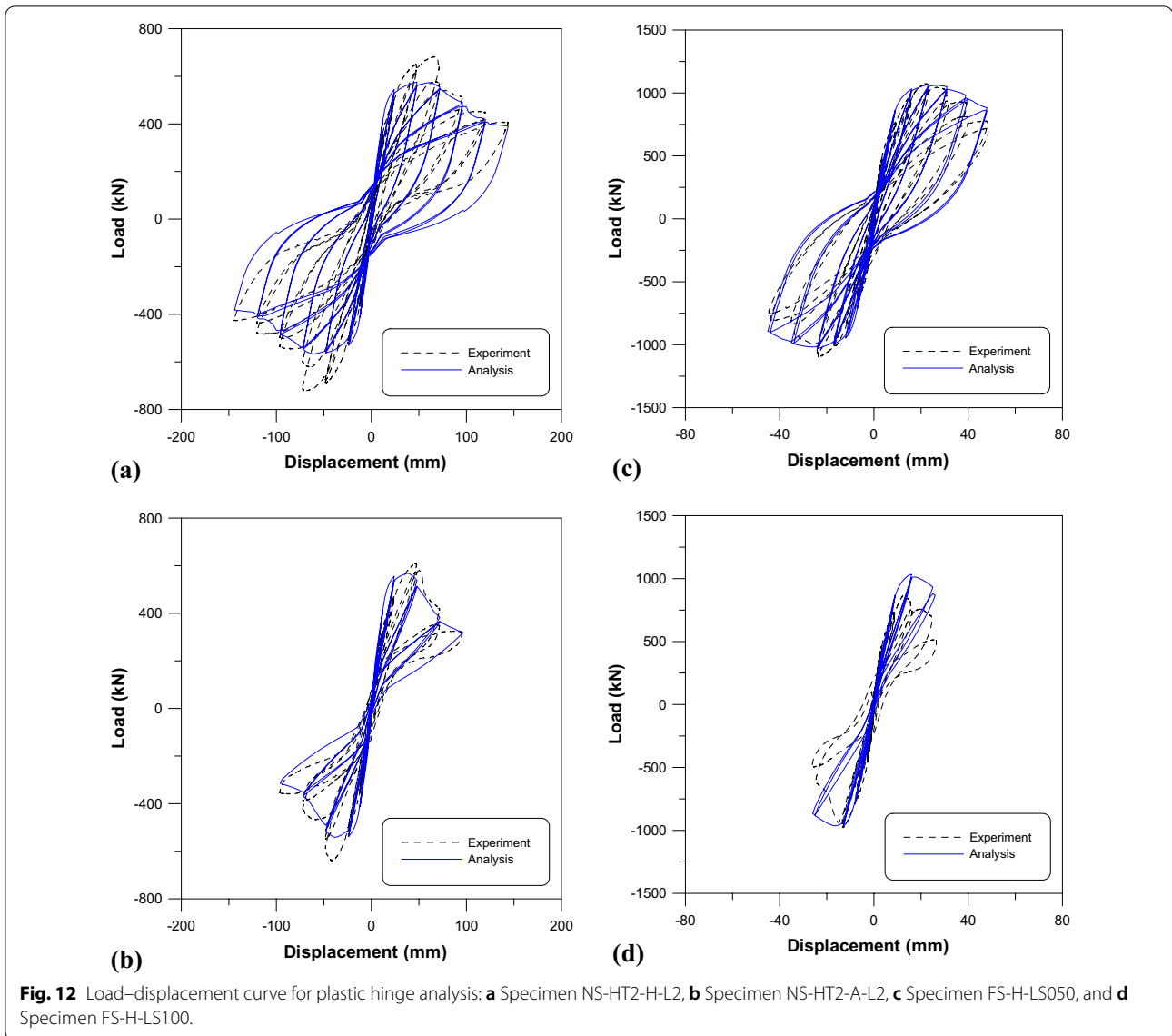


Table 2 Experiment and numerical results.

Specimen	Experiment		Analysis				Ratio of experimental and numerical results			
	V_{max} (kN)	μ_{Δ}	Plane stress analysis		Plastic hinge analysis		Plane stress analysis		Plastic hinge analysis	
			V_{max} (kN)	μ_{Δ}	V_{max} (kN)	μ_{Δ}	V_{max}	μ_{Δ}	V_{max}	μ_{Δ}
NS-HT2-H-L2	682.5	2.6	565.4	3.1	576.0	4.0	1.21	0.84	1.18	0.65
NS-HT2-A-L2	612.1	2.0	561.7	2.3	568.1	2.8	1.09	0.87	1.08	0.71
FS-H-LS050	1075.1	3.0	1067.6	2.1	1069.4	3.1	1.01	1.43	1.01	0.97
FS-H-LS100	869.2	2.5	1001.2	1.5	1034.2	2.5	0.87	1.67	0.84	1.00
Mean							1.04	1.20	1.03	0.83
CV							0.14	0.34	0.14	0.21

Table 3 CPU solved times.

Item	NS-HT2-H-L2	NS-HT2-A-L2	FS-H-LS050	FS-H-LS100
Plane stress analysis				
Total number of elements	83	83	73	73
CPU solved time (seconds)	359.58	131.33	217.72	70.75
Plastic hinge analysis				
Total number of elements	2	2	2	2
CPU solved time (seconds)	59.71	28.69	36.39	13.88

- This novel method can be used for the nonlinear seismic analysis and design of various bridge columns. Efforts should be increased to include certain procedures in the current design codes, such that engineers may develop an acceptable method for evaluating the seismic performance in existing RC bridge columns with lap splices.

Abbreviations

A_c : Cross-sectional area; A_v : Cross-sectional area of shear reinforcement; $B(x)$: Displacement shape function; b_w : Web width of section; $D(x)$: Section force vector; d : Effective depth of section; $d(x)$: Section deformation vector; $\{d_s\}$: Displacement vector; $E(x)$: Fiber stress vector; $e(x)$: Fiber strain vector; E_c : Elastic modulus of concrete; f_{ck} : Characteristic value of cylindrical compressive strength; f_r : Normal stress due to axial force; f_{vs} : Average maximum stress of shear reinforcement considering tension stiffening; f_{vy} : Yield strength of shear reinforcement; G_c : Shear elastic modulus of concrete; G_d : The slope of AB; G_s : The slope of BC; $k_t(x)$: Cross-sectional tangent stiffness matrix; $[k_s]$: Stiffness matrix; L : Height of the column; L_p : Height of the plastic portion; L'_p : Plastic curvatures above the column base; L_{sp} : Length of strain penetration inside the foundation; $M_y(x), M_z(x)$: Bending moment; $N(x)$: Axial force; N_u : Axial force due to factored load; P : Axial load; $\{p_s\}$: Load vector; \bar{Q} : Element force vector; \bar{q} : Element displacement vector; S : Slip; S_0 : Slip at maximum bond stress; S_y : Slip at bar yield; s : Spacing of stirrups; T_e : Element coordinate transformation matrix; V_c : Shear strength without shear reinforcement; V_d : Shear strength with shear reinforcement; V_{max} : Maximum shear force; V_s : Maximum shear force considering tension stiffening; v : Strength reduction factor for concrete cracked in shear; z : Internal arm length along the span; γ : Reduction factor; γ_c : Shear strain; γ_d : Shear strain with shear reinforcement; γ_x : Shear strain considering tension stiffening; $\Delta D_R(x)$: Increment of the section resisting forces; ΔQ_R : Increment of the element resisting forces; Δ_p : Plastic displacement; Δ_u : Ultimate displacement; Δ_y : Yield displacement; $\epsilon(x)$: Axial strain; $\epsilon_{2,d}$: Strain of compressive strut with shear reinforcement; $\epsilon_{2,c}$: Strain of compressive strut considering tension stiffening; ϵ_{cu} : Ultimate strain of concrete; $\bar{\epsilon}_y$: Average yielding strain of shear reinforcement; θ_s : Angle of strut; κ : Shear coefficient; $\kappa_y(x), \kappa_z(x)$: Moment curvatures; μ_Δ : Ductility ratio; τ_b : Bond stress; $\tau_{b,max}$: Maximum bond stress; τ_y : Bond stress at bar yield; ϕ_c : Concrete material resistance factor; ϕ_s : Steel material resistance factor; ϕ_p : Plastic curvature; ϕ_u : Ultimate curvature; ϕ_y : Yield curvature.

Acknowledgements

This work is supported by the Korea Agency for Infrastructure Technology Advancement (KAIA) grant funded by the Ministry of Land, Infrastructure and Transport (Grant 22SGRP-C159279-03). The research described herein was

also sponsored by a grant from R&D Program of the Korea Railroad Research Institute, Republic of Korea.

Author contributions

THK planned this paper, constructed the finite element model, and analyzed the experimental results and the numerical results. KYE analyzed the experimental results and the numerical results. HMS developed the finite element model. All the authors read and approved the final manuscript.

Authors' information

Tae-Hoon Kim, Senior Researcher, Advanced Railroad Civil Engineering Division, Korea Railroad Research Institute, 176, Cheoldobangmulgwan-ro, Uiwang-si, Gyeonggi-do, 16105, Korea.
 Ki-Young Eum, Chief Researcher, Advanced Railroad Civil Engineering Division, Korea Railroad Research Institute, 176, Cheoldobangmulgwan-ro, Uiwang-si, Gyeonggi-do, 16105, Korea.
 Hyun Mock Shin, Emeritus Professor, School of Civil, Architectural Engineering, and Landscape Architecture, Sungkyunkwan University, 2066, Seobo-ro, Suwon-si, Gyeonggi-do, 16419, Korea.

Funding

This work is supported by the Korea Agency for Infrastructure Technology Advancement (KAIA) grant funded by the Ministry of Land, Infrastructure and Transport (Grant 22SGRP-C159279-03). The research described herein was also sponsored by a grant from R&D Program of the Korea Railroad Research Institute, Republic of Korea.

Availability of data and materials

The research data used to support the finding of this study are described and included in the article. Furthermore, some of the data used in this study are also supported by providing references as described in the article.

Declarations

Competing interests

The author declares no competing interests.

Author details

¹Advanced Railroad Civil Engineering Division, Korea Railroad Research Institute, 176, Cheoldobangmulgwan-Ro, Uiwang-Si 16105, Gyeonggi-Do, Korea.
²School of Civil, Architectural Engineering, and Landscape Architecture, Sungkyunkwan University, 2066, Seobo-Ro, Suwon-Si 16419, Gyeonggi-Do, Korea.

Received: 12 April 2022 Accepted: 9 October 2022
 Published online: 12 February 2023

References

- Aboutaha, R. S., Engelhardt, M. D., Jirsa, J. O., & Kreger, M. E. (1999). Experimental investigation of seismic repair of lap splice failures in damaged concrete columns. *ACI Structural Journal*, 96(2), 297–306.
- Alemdar, Z. F. (2010). *Plastic hinging behavior of reinforced concrete bridge columns*, PhD Thesis, University of Kansas, USA.
- Bae, S., & Bayrak, O. (2014). Plastic hinge length of reinforced concrete columns. *ACI Structural Journal*, 105(3), 290–300.
- Bentz, E. C., Vecchio, F. J., & Collins, M. P. (2006). Simplified modified compression field theory for calculating shear strength of reinforced concrete elements. *ACI Structural Journal*, 103(4), 614–624.
- Caltrans (California Department of Transportation). (2010). *Seismic design criteria*, California, CA.
- CEN (Comite Europeen de Normalisation). (2004). *Eurocode 2: EN 1992-1: Design of concrete structures—Part 1: General rules and rules for buildings*. CEN.
- Cerioni, R., Bernardi, P., Michelini, E., & Mordini, A. (2011). A general 3D approach for the analysis of multi-axial fracture behavior of reinforced concrete elements. *Engineering Fracture Mechanics*, 78(8), 1784–1793.
- Darwin, D., Tholen, M. L., Idun, E. K., & Zuo, J. (1996). Splice strength of high relative rib area reinforcing bars. *ACI Structural Journal*, 93(1), 95–107.
- Das, D., & Ayoub, A. (2021). Mixed formulation for geometric and material nonlinearity of shear-critical reinforced concrete columns. *Engineering Structures*, 229, 111587.
- Fedak, L. K. (2012). *Evaluation of plastic hinge models and inelastic analysis tools for performance-based seismic design of RC bridge columns*. Michigan State University.
- Han, Q., Zhou, Y.-L., Du, X., Huang, C., & Lee, G. C. (2014). Experimental and numerical studies on seismic performance of hollow RC bridge columns. *Earthquakes and Structures*, 7(3), 251–269.
- Kim, T.-H., Lee, K.-M., Yoon, C.-Y., & Shin, H. M. (2003). Inelastic behavior and ductility capacity of reinforced concrete bridge piers under earthquake. I: Theory and formulation. *Journal of Structural Engineering, ASCE*, 129(9), 1199–1207.
- Kim, T.-H. (2022). Seismic performance assessment of deteriorated two-span reinforced concrete bridges. *International Journal of Concrete Structures and Materials*, 16(2), 123–135.
- Kim, T.-H., Hong, H.-K., Chung, Y.-S., & Shin, H. M. (2009). Seismic performance assessment of reinforced concrete bridge piers with lap splices using shaking table tests. *Magazine of Concrete Research*, 61(9), 705–719.
- Kim, T.-H., Kim, B.-S., Chung, Y.-S., & Shin, H. M. (2006). Seismic performance assessment of reinforced concrete bridge piers with lap splices. *Engineering Structures*, 28(6), 935–945.
- Kim, T.-H., Lee, J.-H., & Shin, H. M. (2014). Performance assessment of hollow reinforced concrete bridge columns with triangular reinforcement details. *Magazine of Concrete Research*, 66(16), 809–824.
- Mander, J. B., Priestley, M. J. N., & Park, R. (1988). Theoretical stress-strain model for confined concrete. *Journal of Structural Engineering, ASCE*, 114(8), 1804–1826.
- Marini, A., & Spacone, E. (2006). Analysis of reinforced concrete elements including shear effects. *ACI Structural Journal*, 103(5), 645–655.
- MCT (Ministry of Construction and Transportation). (2012). *Korea bridge design code (limit state design method)*. MCT.
- Michelini, E., Bernardi, P., & Cerioni, R. (2017). Failure analysis of RC beams subjected to shear through different numerical approaches. *Engineering Failure Analysis*, 82, 229–242.
- Mirzabozorg, H., & Ghaemian, M. (2005). Non-linear behavior of mass concrete in three-dimensional problems using a smeared crack approach. *Earthquake Engineering and Structural Dynamics*, 34(3), 247–269.
- Moshirabadi, S., & Soltani, M. (2019). Implementation of smeared crack approach in rigid block and spring modeling of reinforced concrete. *Engineering Structures*, 201(3), 109779.
- Mourlas, C., Markou, G., & Papadrakakis, M. (2017). 3D nonlinear constitutive modeling for dynamic analysis of reinforced concrete structural members. *Procedia Engineering*, 199, 729–734.
- Mullapudi, T. R., & Ayoub, A. (2010). Modeling of the seismic behavior of shear-critical reinforced concrete columns. *Engineering Structures*, 32, 3601–3615.
- Mullapudi, T. R., & Ayoub, A. (2018). Fiber beam analysis of reinforced concrete members with cyclic constitutive and material laws. *International Journal of Concrete Structures and Materials*, 12(6), 885–900.
- Spiliopoulos, K. V., & Lykidis, G. C. (2006). An efficient three-dimensional solid finite element dynamic analysis of reinforced concrete structures. *Earthquake Engineering and Structural Dynamics*, 35(2), 137–157.
- Taylor, R. L. (2000). *FEAP—A finite element analysis program, version 7.2 users manual, Volume 1 and 2*, University of California at Berkeley.
- Vecchio, F. J. (2000). Disturbed stress field model for reinforced concrete: Formulation. *Journal of Structural Engineering, ASCE*, 126(9), 1070–1077.
- Xu, J.-G., Feng, D.-C., Wu, G., Cotsosovos, D. M., & Lu, Y. (2020). Analytical modeling of corroded RC columns considering flexure-shear interaction for seismic performance assessment. *Bulletin of Earthquake Engineering*, 18, 2165–2190.
- Zendaoui, A., Kadid, A., & Yahiaoui, D. (2016). Comparison of different numerical models of RC elements for predicting the seismic performance of structures. *International Journal of Concrete Structures and Materials*, 10(4), 461–478.
- Zhu, R. R. H., Hsu, T. T. C., & Lee, J. Y. (2001). Rational shear modulus for smeared-crack analysis of reinforced concrete. *ACI Structural Journal*, 98(4), 443–450.

Publisher's Note

Springer Nature remains neutral with regard to jurisdictional claims in published maps and institutional affiliations.

Submit your manuscript to a SpringerOpen® journal and benefit from:

- Convenient online submission
- Rigorous peer review
- Open access: articles freely available online
- High visibility within the field
- Retaining the copyright to your article

Submit your next manuscript at ► [springeropen.com](https://www.springeropen.com)